https://doi.org/10.15407/exp-oncology.2023.04.493

L. Miroshnichenko [1, *], L. Vasiliev [1], G. Shustakova [2], E. Gordiyenko [2], Yu. Fomenko [2], I. Dunaieva [3]

[1] State Institution «Grigoriev Institute for Medical Radiology and Oncology of the National Academy of Medical Sciences of Ukraine», Kharkiv, Ukraine
[2] B. Verkin Institute for Low Temperature Physics and Engineering of the National Academy of Sciences of Ukraine, Kharkiv, Ukraine
[3] Kharkiv National Medical University, Kharkiv, Ukraine
* Correspondence: Email: lumira78@gmail.com

INFRARED THERMAL IMAGING CONTROL OF RADIATION DERMATITIS DYNAMICS

Background. Radiation-induced dermatitis impairs the quality of life of cancer patients and may lead to the need of interrupting radiotherapy. The grade of dermatitis is subjectively assessed by the visual examination. There is an urgent need for both objective and quantitative methods for assessing the current grade of dermatitis and predicting its severity at an early stage of radiotherapy. **Aim.** The aim of the study was to evaluate the advantages and limitations of infrared thermography for monitoring the current level of radiation-induced dermatitis and predicting its severity by quantitative analysis of the thermal field dynamics in the irradiated zone. **Materials and Methods.** 30 adult patients were examined by infrared thermography during the course of 2D conventional radiotherapy for malignant tumors of various types and localizations. Our approach for quantifying the thermal field caused by dermatitis alone was applied. A statistical (correlation and ROC) analysis was performed. **Results.** Dermatitis of varying severity was observed in 100% of the patients studied. The dynamics in the intensity of the anomalous thermal fields in the irradiated zone correlated with the dynamics of dermatitis grades, excluding the case of a radiosensitive tumor (correlation coefficient 0.74÷0.84). It was found that the maximum toxicity (dermatitis grade ≥ 3) develops in patients who how significant hyperthermia in the area of interest (≥ 0.7 °C) at an early stage of radiotherapy. The ROC analysis demonstrated the "good quality" of the prognosis method (AUC = 0.871). **Conclusions.** The non-invasive and cheap infrared thermography is a suitable tool for objective quantitative monitoring the current dermatitis grade during radiotherapy as well as predicting its severity for any tumor location.

Keywords: oncology, radiation therapy, dermatitis, thermography.

Citation: Miroshnichenko L, Vasiliev L, Shustakova G, Gordiyenko E, Fomenko Yu, Dunaieva I. Infrared thermal imaging control of radiation dermatitis dynamics. *Exp Oncol*. 2023; 45(4): 493-503. https:// doi.org/10.15407/exp-oncology.2023.04.493

Radiation therapy (RT) has two serious and painful local side effects: radiation-induced dermatitis (RID) and radiation-induced mucositis (RIM) [1—3]. RID is caused by radiation damage to the skin and subcutaneous tissue, while RIM is caused by mucosal damage. Both side effects worsen the quality of cancer patient life and may lead to the need to interrupt RT.

RID is a common side effect of RT. It is believed to develop during the course of RT in an average of 95% of patients. It develops in 74%—100% of patients with breast cancer (BC) and in 80%—90% of patients with head and neck cancer (HNC); of these, severe skin reactions develop in 25% of patients [1]. Every third patient suffers from chronic RID [4]. There are also reports on recurrent RID [5], an acute inflammatory skin reaction in a previously irradiated area caused by the intake of a chemotherapeutic agent.

The main symptoms of RID are pain, itching, burning, swelling, ulceration, associated infections, and psychological discomfort. The acute phase of RID lasts 90 days from the start of RT. Skin damage usually appears within the first 24 h after the start of RT as a transient erythema. During the following 2—4 weeks of RT, more persistent generalized erythema and other skin changes (dryness and hyperpigmentation) appear causing painful sensations. Subsequently (3—6 weeks from the start of RT), moist desquamation may develop. In this case, a temporary cessation of RT is sometimes required until the epithelium is restored. In 90 days after the end of RT ends, chronic RID may occur and persist for years. This phase is characterized by vascular damage, telangiectasia, fibrosis, edema, epidermal thinning, dermal atrophy, keratosis, and even dermal necrosis. There is an increased risk of non-melanoma malignant skin neoplasms in this phase [4].

The severity of RID depends on two groups of risk factors. The first group includes "objective parameters", such as the type of equipment, parameters of the RT regimen, tumor localization (irradiation zone and volume), single and total doses of radiation, duration of RT, and concomitant systemic treatment. It would seem that these factors can suggest an approximate level of RID [6]. In practice, patients have a significant individual variation in the RID dynamics, even with identical tumor characteristics and treatment regimens. This is explained by the presence of "subjective" risk factors due to the individual characteristics of the patient: excessive BMI, skin diseases such as psoriasis, etc. However, the main subjective risk factor for severe toxicity is the patient's genetic predisposition, which makes it almost impossible to predict the RID severity to take preventive measures. Therefore, constant monitoring of the RID dynamics is necessary to make timely adjustments to local and systemic treatment, as well as change, if necessary, in the RT regimen.

The severity of RID is periodically assessed by an oncologist according to the standard "Common Terminology Criteria for Adverse Events (CTCAE)" [7]. As a result of a visual examination of the irradiated area, the clinician assigns an integer value from 0 to 4 to the current RID level. RID = 0 corresponds to the absence of dermatitis, and RID = 4 is the maximum damage to the skin and subcutaneous tissue, at which RT is interrupted in 100% of cases. It is clear that the visual examination is quite subjective, so the existing method of RID level evaluation has a significant error.

Therefore, there is a need for an objective quantitative method for assessing the current level of RID, as well as an urgent need for a predictive method for assessing the expected RID severity at an early stage of treatment.

A non-invasive, cheap, and easy-to-use infrared thermography (IRT) [8—10] is a suitable method for quantitative control of RID dynamics since one of the main features of RID is an anomalous thermal field on the skin surface.

Most researchers use IRT to study the RID dynamics during RT of one of the breasts [11—14].

In this case, the criterion of disturbing the "normal" thermal symmetry is used to quantify the dynamics of hyperthermia in the irradiated zone, and the reference area is located on the healthy breast symmetrically to the area of interest. However, at other tumor locations, difficulties arise with the choice of the reference area. Also, hyperthermia caused by RID can be superimposed by hyperthermia caused by RIM. To quantify RID-induced hyperthermia, it is also important to take into account the dynamics of the tumor's own "thermal imprint" in the area of interest.

The study is aimed to evaluate the advantages and limitations of IRT for monitoring the current level of RID and predicting its severity by quantifying the thermal field dynamics in the irradiated zone of tumors of various locations and types.

Materials and Methods

Patient data. The study involved 30 adult patients who received a full course of conventional 2D RT using a Theratron Elite-80 gamma-therapy device [15]. The condition for patients enrolling in the study was the absence of prior RT and concomitant chemotherapy. Patients received the standard skin care strategy, but no later than 6 h before the study. Of the entire cohort, 16 patients had HNC, of them 12 had tumors of the ENT-organs (larynx, tonsils, tongue, vocal cords, etc.). 8 patients had BC, and 6 had tumors of other organs (gastrointestinal tract or lungs). The study involved 13 (43%) women and 17 (57%) men aged 30 to 72 years.

The study has been carried out by the World Medical Association Code of Ethics (Declaration of Helsinki) for experiments involving humans. A non-invasive examination of patients was carried out at the Kharkiv Regional Clinical Oncological Center and the State Institution "Grigoriev Institute for Medical Radiology and Oncology of the NAMS of Ukraine" with the approval of the ethics committees of these institutions. Each patient gave written informed consent to participate in the research.

Radiation doses. Thermal imaging examination of patients was carried out during the first stage of RT, which consisted of 4 cycles of daily exposures (5 days each) with a 2-day break between the cycles. Depending on the type, location, and stage of the tumor, as well as taking into account the medical history and health status, patients received the standard schemes for irradiation:

- Larynx: single radiation dose SRD ≈ (2—3) Gy. The total radiation dose TRD ≈ 40 Gy;
- Skin: SRD ≈ (2—4) Gy, TRD ≈ 40 Gy;
- Pancreas, lungs, and other internal organs: SRD ≈ (2—3) Gy, TRD ≈ 40 Gy;
- Breast: SRD ≈ (2—3) Gy, TRD ≈ (40÷60) Gy on the primary site, and TRD ≈ 40 Gy on the path of lymph outflow (axillary, subclavian lymph nodes, parasternal (or sternal) field).

Thermal data processing. The study of the thermal field dynamics in the irradiated zone was carried out by a method of passive IRT. A thermal field analyzer based on an uncooled array (384 × 288) of microbolometers was used [16]. The device features a spectral range of 8—14 micrometers, temperature sensitivity of 0.07 °C, spatial resolution of 1 milliradian, and an original software package specialized for medical applications. Before the study, the device was tested in a metrological bench Fluke Portable Infrared Calibrator-9133 (Fluke Corporation, USA) [17].

The thermal imaging examination of patients was carried out in a special room in compliance with the climatic requirements and rules for preparing patients.

Each patient underwent an examination before the RT start (baseline session) and 4 times before the start of each RT cycle. At each thermal imaging session, the clinician determined the current grade of RID by the results of the visual examination of the irradiation zone and patient questioning about felt symptoms of RID (burning, tension, etc.).

A relative temperature scale was used to assess the dynamics of the thermal fields, with the reference temperature area selected in the non-irradiated zone individually for each patient depending on the tumor localization. The simple procedure for quantifying the dynamics of the abnormal thermal field caused by the RID is described in [18].

An area of interest (ai) and a reference area (ref) were selected for each patient at the baseline thermal imaging session (session #0, before RT start) and remained unchanged for the patient during subsequent monitoring. The area of interest was always located in the irradiated zone and coincided with it in shape and size. When choosing a reference area, a criterion of disturbing the "normal" thermal symmetry was used if possible. In this case, both areas were symmetrical, contralateral, and equal in shape and area. If it was not possible to use this generally accepted approach, a reference area of acceptable size was chosen in adjacent healthy tissues, but not closer than 3 cm from the edge of the zone of possible hyperthermia. The baseline relative temperature in the area of interest for each patient was calculated as:

$$\Delta(T_{ai})_0 = (T_{ai})_0 - (T_{ref})_0 \quad (1)$$

Similarly, the relative temperature of the area of interest measured in each subsequent thermal imaging session was:

$$\Delta(T_{ai})_j = (T_{ai})_j - (T_{ref})_j \quad (2)$$

where j is the number of the current thermal imaging session. The reduced relative temperature of the area of interest was calculated as follows:

$$\delta(T_{ai})_j = \Delta(T_{ai})_j - \Delta(T_{ai})_0 \quad (3)$$

The use of $\delta(T_{ai})_j$ made it possible to exclude from the analysis of the thermal field caused by RID's other effects such as the tumor's own thermal imprint, hyperthermia caused by postoperative inflammatory processes, etc.

The dynamics of $\delta(T_{ai})_j$ was compared with the dynamics of the RID grade for each patient. We estimated the absolute error of relative temperature measurement as ±0.1 °C and the clinical assessment of RID as ±0.5.

Statistical methods of clinical practice were applied by [19], using Statistica 10 (StatSoft, USA) and Excel 2010 software (Microsoft, USA).

Results and Discussion

Commonly used data processing. We used the criterion of disturbing thermal symmetry to quantify the dynamics of thermal fields in the area of interest by the generally accepted approach [11—14]. However, given the various locations of tumors (areas of interest), it was possible to apply it only to 11 patients (37%), including all patients with BC. A typical example is shown in Fig. 1. The baseline thermogram of the patient's torso after the radical sectoral resection of a malignant neoplasm of the right breast ($T_2N_0M_0$) is shown in Fig. 1, *a*. The black rectangle on the thermogram (Fig. 1, *a*) shows the area of interest on the right breast coinciding with the irradiation area (10 × 15) cm^2, and the white rectangle marks the symmetrical reference area on the healthy breast. The thermogram of the breast after TRD = 30 Gy is shown in Fig. 1, *b*. As seen, the region of hyperthermia significantly exceeds the irradiated zone. Both the dynamics of the reduced relative temperature in the area of interest (solid line) and the change in the RID grade (separate points) during RT are shown in Fig 1, *c*. For this case, the correlation coefficient $r[\delta(T_{ai})\text{: RID}] = 0.978$.

In cases where this approach could not be applied, the reference region was selected individually in the adjacent healthy tissues.

Radiosensitive tumor. According to our approach to quantifying obtained thermograms, we subtract the "thermal imprint" of the tumor itself, assuming that the changes in the tumor's temperature due to RT are significantly less than

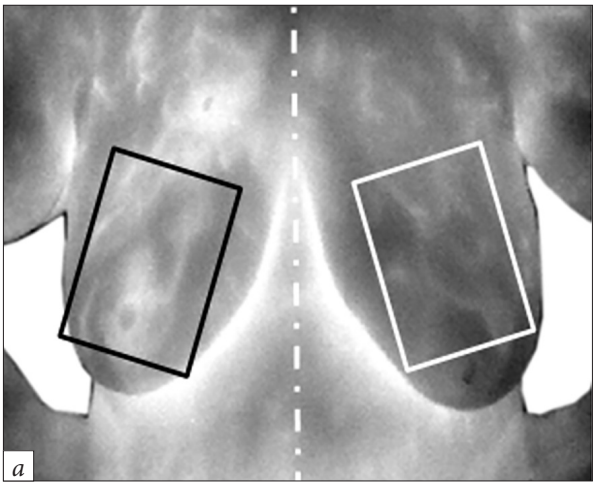

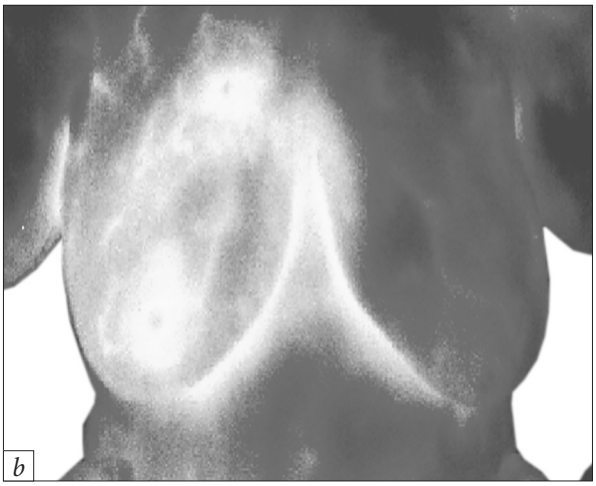

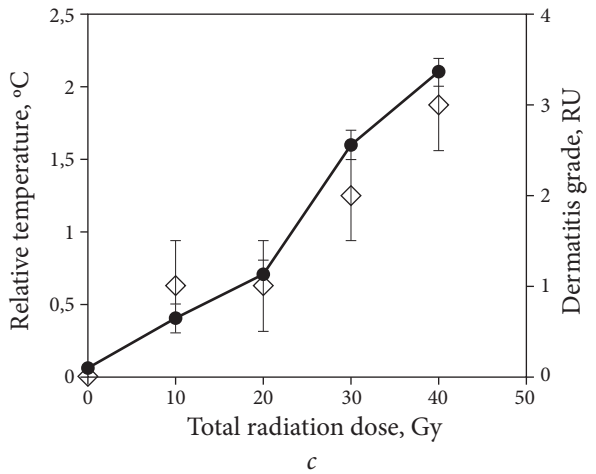

Fig. 1. Dynamics of the anomalous thermal field during RT: *a*) baseline thermogram of the patient torso with right breast cancer $T_2N_0M_0$ with marked area of interest and reference area; *b*) thermogram after TRD = 30 Gy; *c*) changes in the relative temperature and RID grade during RT

the rise of hyperthermia caused by RID. However, this assumption may be false for radiosensitive tumors. The baseline thermogram of the inguinal region of the patient with inguinal stage III non-Hodgkin MALT lymphoma is shown in Fig. 2, *a*. The patient was prescribed a course of RT of the right inguinal-femoral-iliac lymph node (SRD = 2 Gy, TRD = 40 Gy). The area of interest (black square on the thermogram) coincides with the irradiated zone (20 × 20) cm^2. The reference area (white square) is based on the large zone of irradiation. Before RT starts, $\Delta(T_{ai})_0$ = 3.1 °C, that is, lymphoma is well diagnosed by IRT. A significant (≈ 2 °C) decrease in the relative temperature during the first 2 weeks of RT and a further increase starting from the third week of RT are observed (Fig. 2, *b*). Presumably, this is the manifestation of two simultaneous processes: the reduction of the "thermal imprint" of the tumor on the skin as a result of tumor regression and the parallel development of minor RID. Both processes are confirmed clinically: RID = (0, 1, 2, 2, 2) was assessed by the doctor, and ultrasound showed a regression of the tumor diameter due to RT from 18 to 10 cm.

Using IRT, we cannot separate the dynamics of the "thermal imprint" of the tumor from the growth of hyperthermia caused by RID, because we do not know the current temperature of the tumor itself. Clinical imaging methods (MRI, CT, and ultrasound) provide information only about the shape and size of the tumor, but not

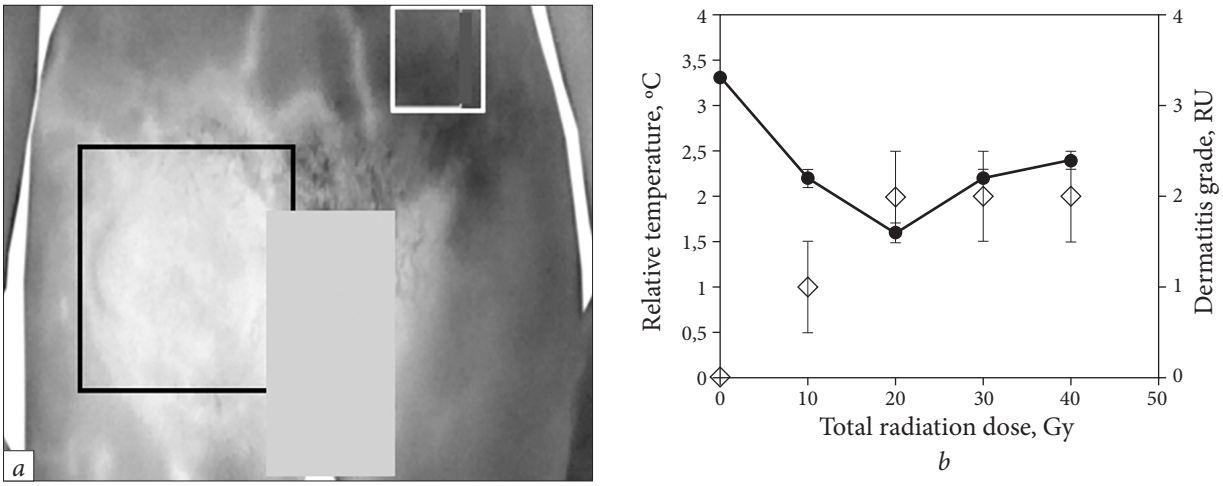

Fig. 2. Dynamics of hyperthermia with simultaneous RID development and radiosensitive tumor regression (inguinal non-Hodgkin's MALT-lymphoma stage III): *a*) baseline thermogram with marked area of interest and reference area (black and white squares, respectively); *b*) relative temperature dynamics in the area of interest (solid curve) and RID grade (points)

about tumor temperature. However, research in this direction is already underway [20].

Thus, IRT cannot be used to directly control the RID dynamics in the case of radiosensitive tumors. However, it should be noted that a high level of tumor radiosensitivity was observed only in one patient from the entire cohort.

Thermal field caused by RID + RIM. When analyzing the dynamics of thermal fields caused by RID in patients with HNC, we encountered two methodological difficulties. Firstly, there was a need to optimally choose the reference area, since the neck is irradiated from two sides in most cases. This makes it impossible to use the thermal symmetry criterion. Secondly, abnormal thermal fields in the area of interest are due to the development of both RID and RIM, and RIM is significant in these tumor localizations [21]. Previously, we used the outer surface of the lower lip as the area of interest, and the nose bridge as the reference area to analyze the hyperthermia caused by RIM in HNC patients [22]. Here, we used the irradiation zone as the area of interest and the lower lip area (5 × 2) cm^2 as the reference area for RID analysis. We assumed that RIM on the mucous membrane of the lip develops in the same way as RIM on the mucous membrane of the larynx. This approach allowed us to analyze the dynamics of hyperthermia caused by RID alone, subtracting the hyperthermia caused by RIM. An example is shown in Fig. 3.

The thermograms of a patient with squamous cell keratinizing cancer of the larynx on the right $T_3N_0M_0$ are shown in Fig. 3, *a*, *b*. On the baseline thermogram (Fig. 3, *a*), the black rectangle shows the area of interest, which coincides with the irradiation zone (8 × 12) cm^2, and the white rectangle is the reference area. The thermogram (Fig. 3, *b*) qualitatively illustrates the growth of the area of hyperthermia caused by RID + RIM after TRD = 40 Gy. The dependence of the reduced relative temperature in the area of interest on the received dose (solid curve) and the corresponding values of the RID grade (points) are shown in Fig. 3, *c*. For this case, r = 0.964. Also, for comparison, the graph shows the dynamics of the hyperthermia induced jointly by RID + + RIM (dashed curve). Here, the site of the eyelid in the region of the nose bridge is chosen as the reference area.

Statistical analysis. When analyzing the thermal and clinical data of 30 examined patients,

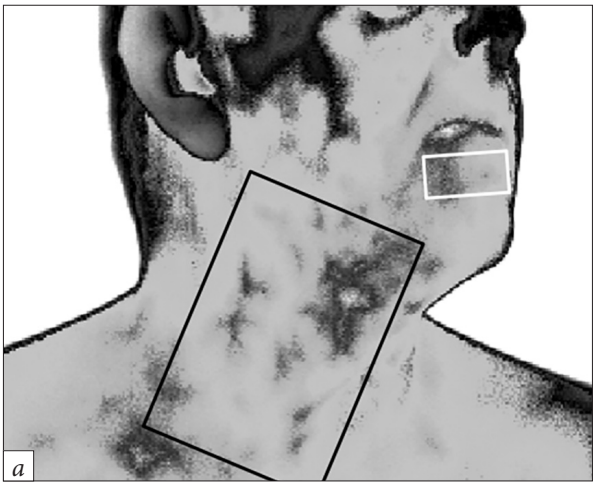

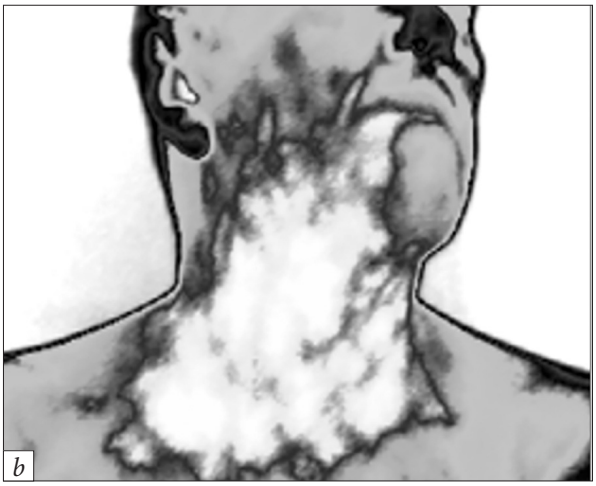

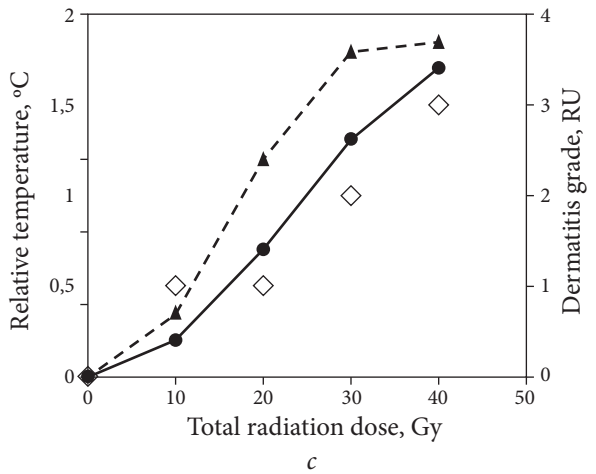

Fig. 3. Dynamics of hyperthermia with the simultaneous development of RID and RIM in a patient with keratinizing cancer of the larynx on the right $T_3N_0M_0$: *a*) baseline thermogram with marked area of interest (irradiated zone) and reference area (black and white rectangles, respectively); *b*) thermogram after 40 Gy; *c*) dynamics of relative temperature in the area of interest (solid curve) and RID grade (points). The dotted curve illustrates the dynamics of hyperthermia induced by RID + RIM together

we formulated hypotheses about the presence of a correlation between the value of the reduced relative temperature and the RID grade at each IRT session, as well as between the value of the reduced relative temperature obtained at the first IRT session and the maximum RID grade. A correlation analysis was used and a regression model was built to test these hypotheses. Table 1 presents the correlation coefficients $r[\delta(T_{ai})_j : RID_j]_{1...30}$ obtained for each of the four IRT sessions.

Given the rather high degree of correlation between the values of the reduced relative temperatures and the degree of RID at each session, a regression model was built (with a significance level of 0.05) to control the RID severity by temperature parameters (Fig. 4). The coefficient of linear determination of the obtained

Table 1. **Pearson's correlation coefficient between the reduced relative temperatures and the corresponding RID grades at IRT sessions j =1...4**

j	1	2	3	4
Correlation coefficient *p*	0.737 0.000003	0.772 0.0000006	0.803 0.0000001	0.836 0.000000009

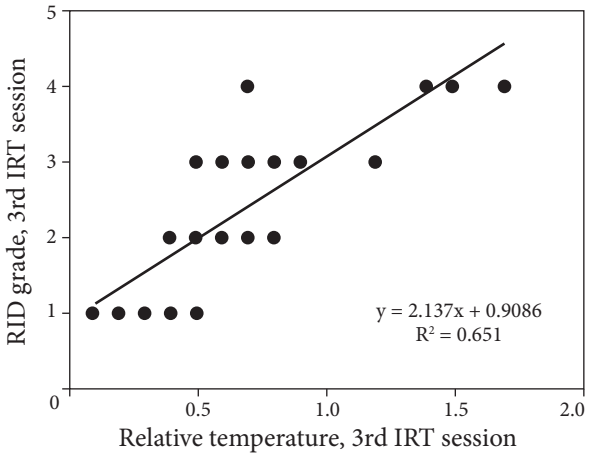

Fig. 4. Regression model of the relationship between thermal parameters and clinical indicators (RID grade) for the 3rd IRT session

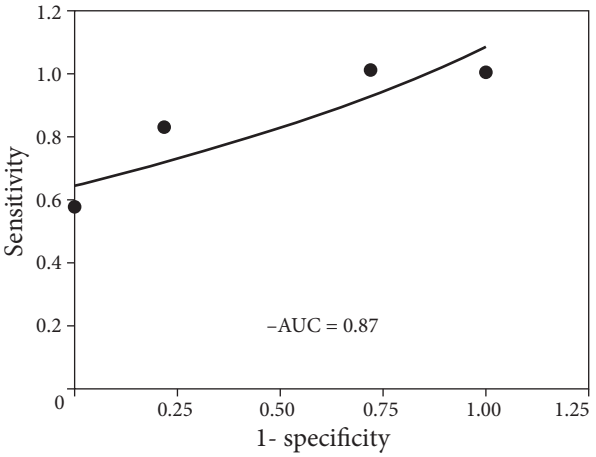

Fig. 5. A receiver operation characteristic curve

model $R^2 = 0.651$ indicates the acceptability of the model and a satisfactory approximation, although it does not show the absolute adequacy of the model to the described process.

The correlation coefficient $r[\delta(T_{ai})_1 : RID_4]_{1...30} = 0.828$ ($p = 0.00000002$) was obtained for the values of the reduced relative temperatures obtained at the first IRT session (j = 1) and the maximum RID grades (j = 4). Considering the discrete ordinal nature of the RID grade data, the Spearman nonparametric correlation method was used to clarify the presence and nature of the dependence. As a result, Spearman's rank correlation coefficient ρ is equal to 0.849. The relationship between the studied traits is direct, and the strength of the connection according to the Chaddock scale is high. The critical value of the Spearman criterion at 28 degrees of freedom is 0.362, that is, $\rho_{obs} > \rho_{crit}$, which means that the dependence of the signs is statistically significant ($p < 0.05$).

Based on these results, a predictive diagnostic model was proposed to predict the RID severity by the degree of hyperthermia in the area of interest at the first IRT session. To build a predictive method, the optimal cut-off value, $\delta(T_{ai})_1 = 0.7$ °C, was found. Thus, a high level of toxicity (RID = 3+...4) develops in patients who have severe hyperthermia in the area of interest $\delta(T_{ai})_1 \geq 0.7$ °C at the first IRT session (after TRD ≈ 10 Gy). A model with such a cut-off value has balanced sensitivity and specificity values, as well as a fairly high accuracy (Table 2).

In Table 2, a is a true positive result, b is a pseudo positive result, c is a true negative result, and d is a pseudo negative result. Thus, we obtained: the sensitivity = a/(a + b) = 0.83, the specificity = d/(d + c) = 0.78, and the accuracy = = (a + d)/(a + b + c + d) = 0.80. The subsequent ROC analysis (Fig. 5) showed the good quality of the predictive method (AUC = 0.871).

Chronic RID. Additionally, a thermal imaging examination of individual patients with RID in the chronic phase was performed (these patients

Table 2. **Conjugation table for assessing information content of diagnostic test**

Number of patients with: / Thermal parameter	Presence of high-grade RID (RID ≥ 3)	Absence of high-grade RID (RID < 3)
$\delta(T_{ai})_1 \geq 0.7$ °C	10 (a)	4 (c)
$\delta(T_{ai})_1 < 0.7$ °C	2 (b)	14 (d)
Total	12	18

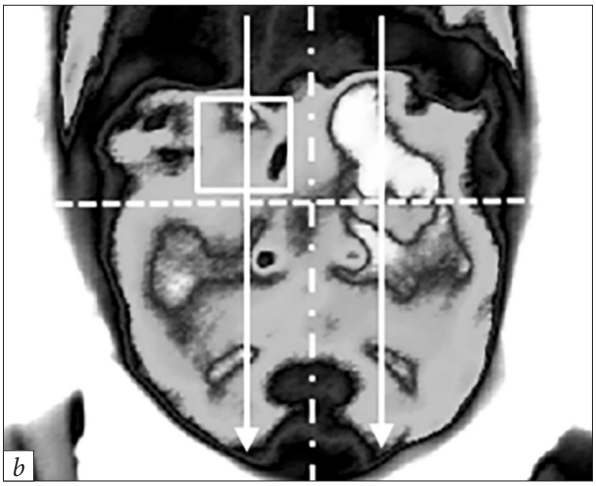

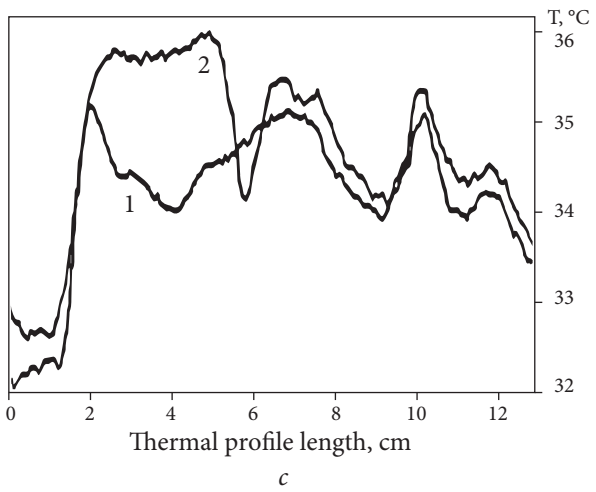

Fig. 6. Thermal imaging detection of complications in chronic RID: *a*) photo of the patient's face with a visible lesion of the cheek skin (radiation burn); *b*) thermogram of the face with hyperthermia over the burn: the lower thermo-symmetric part is separated by a horizontal dotted line, the reference area is marked with a square, and the thermal profile positions are indicated by arrows; *c*) thermal profiles from top to bottom according to the arrows

were not included in the cohort). As an example, Fig. 6 illustrates the results of the examination of the patient 9 months after RT for basal cell carcinoma on the skin of the left cheek $T_1N_0M_0$ (TRD = 60 Gy on zone (4 × 4) cm^2). In the photo of the patient's face (Fig. 6, *a*), you can see damage to the cheek skin at the RT zone (radiation burn). However, the thermogram (Fig. 6, *b*) shows good thermal symmetry in the lower part of the face (below the dotted line). It indicates the absence of significant inflammatory (hyperthermia) or necrotic (hypothermia) processes in the former irradiated zone. At the same time, significant hyperthermia is observed above the irradiated zone. Thermal symmetry distortion $\Delta(T_{ai}) = (T_{ai}) - (T_{ref}) \approx 1.0$ °C. The thermal symmetry in the lower part of the face and the thermal asymmetry above it are also confirmed by the thermal profiles drawn from top to bottom through the area of interest and the reference area (Fig. 6, *c*). Presumably, current inflammation is caused by the use of an inappropriate drug for chronic RID treatment. The dynamics of the parameter $\Delta(T_{ai})$ can be a quantitative criterion of treatment adequacy.

To sum up, the results of monitoring the dynamics of the abnormal thermal fields in the irradiated zones of the patient skin during RT, and the analysis of the thermal data according to the proposed algorithm have demonstrated that

- RID of varying degrees of severity was observed in 100% of patients studied.

• The increase in the intensity of abnormal thermal fields in the irradiated zone correlates with the dynamics of RID: r = (0.74÷0.84) for most types and localizations of tumors. The exception is radiosensitive tumors since at the moment, we cannot take into account the contribution of the tumor "thermal imprint" dynamics to the dynamics of RID-induced hyperthermia.

• A high level of toxicity (RID = 3+, 4) develops in patients with significant hyperthermia in the area of interest (≥ 0.7 °C) at the early stage of RT. The indicator of "good quality" of the proposed predictive method (AUC = 0.871) was obtained.

• The proposed approach to quantify thermal data allows monitoring the dynamics of RID only, even in areas with a significant RIM. However, this approach is based on the clinically unproven assumption that the level of RIM is the same in the mucosa under the irradiated zone (for example, larynx) and in the nearby but not irradiated site (lower lip).

• IRT can be successfully used for monitoring complications (inflammation, blood circulation disorders, necrosis, etc.) in the chronic phase of RID.

We should note that the results were obtained on samples of insufficient statistical power, and further research in this direction is needed to confirm the results. Nevertheless, the non-invasive and cheap IRT method is a suitable tool for the objective quantitative monitoring of RID.

Funding sources

National Academy of Sciences of Ukraine, grant 0114U002775.

Declaration of competing interest

None.

REFERENCES

1. Iacovelli NA, Torrente Y, Ciuffreda A, et al. Topical treatment of radiation-induced dermatitis: current issues and potential solutions. *Drugs Context*. 2020;9:2020-4-7. https://doi.org/10.7573/dic.2020-4-7
2. Maria OM, Eliopoulos N, Muanza T. Radiation-induced oral mucositis. *Front Oncol*. 2017;7:89. https://doi.org/10.3389/fonc.2017.00089
3. Rades D, Narvaez CA, Doemer C, et al. Radiotherapy-related skin toxicity (RAREST-02): A randomized trial testing the effect of a mobile application reminding head-and-neck cancer patients to perform skin care (reminder app) on radiation dermatitis. *Trials*. 2020;21:424. https://doi.org/10.1186/s13063-020-04307-0
4. Spałek M. Chronic radiation-induced dermatitis: challenges and solutions. *Clin Cosmet Investig Dermatol*. 2016;9:473-482. https://doi.org/10.2147/CCID.S94320
5. Burris HA 3rd, Hurtig J. Radiation recall with anticancer agents. *Oncologist*. 2010;15(11):1227-1237. https://doi.org/10.1634/theoncologist.2009-0090
6. Kawamura M, Yoshimura M, Asada H, et al. A scoring system predicting acute radiation dermatitis in patients with head and neck cancer treated with intensity-modulated radiotherapy. *Radiat Oncol*. 2019;14:14. https://doi.org/10.1186/s13014-019-1215-2
7. The Common Terminology Criteria for Adverse Events (CTCAE) ver. 4.0. Publication date: June 14, 2010. https://ctep.cancer.gov/protocoldevelopment/electronic_applications/ctc.htm.
8. Glushchuk NI, Gordiyenko EYu, Fomenko YuV, et al. The results of the study of human anomalos thermal fields under irradiation. *Sci Innov*. 2017;13(2):43-52. https://doi.org/10.15407/scine13.02.043
9. Hoffer OA, Ben-David MA, Katz E, et al. Thermal imaging as a tool for evaluating tumor treatment efficacy. *J Biomed Opt*. 2018;23(5):058001. https://doi.org/10.1117/1.JBO.23.5.058001
10. Shaikh S, Akhter N, Manza R. Current trends in the application of thermal imaging in medical condition analysis. *IJITEE*. 2019;8(8):2708-2712. https://www.ijitee.org/wp-content/uploads/papers/v8i8/F5073048619.pdf
11. Zhu W, Jia L, Chen G, et al. Relationships between the changes of skin temperature and radiation skin injury. *Int J Hyperthermia*. 2019;36(1):1159-1166. https://doi.org/10.1080/02656736.2019.1685685
12. Maillot O, Leduc N, Atallah V, et al. Evaluation of acute skin toxicity of breast radiotherapy using thermography: Results of a prospective single-centre trial. *Cancer Radiother*. 2018;22(3):205-210. https://doi.org/10.1016/j.canrad.2017.10.007

13. Saednia K, Tabbarah S, Lagree A, et al. Quantitative thermal imaging biomarkers to detect acute skin toxicity from breast radiation therapy using supervised machine learning. *Int J Radiat Oncol Biol Phys*. 2020;106(5):1071-1083. https://doi.org/10.1016/j.ijrobp.2019.12.032
14. Baic A, Plaza D, Lange B, et al. The use of thermal imaging in the evaluation of temperature effects of radiotherapy in patients after mastectomy-first study. *Sensors*. 2021;21:7068. https://doi.org/10.3390/s21217068
15. THERATRON ELITE 80. https://medicaldevices.icij.org/devices/can-theratron-elite-80-6fce1e91
16. Gordienko EYu, Glushchuk NI, Pushkar' YuYa, et.al. A multielement thermal imaging system based on an uncooled bolometric array. *Instrum Exp Tech*. 2012;55(4):494-497. https://doi.org/10.1134/S0020441212030050
17. Fluke 9132/9133 Portable Infrared Calibrator. https://www.fluke.com/en-us/product/calibration-tools/temperature-calibrators/fluke-calibration-9132-9133
18. Kiporenko PV, Gordiyenko EYu, Fomenko YuV, Shustakova GV. The procedure for measurement of the human temperature field dynamics. *Ukr Metrol J.* 2018;3:62-66. https://doi.org/10.24027/2306-7039.3.2018.153131
19. Rumyantsev PO, Saenko UV, Rumyantseva UV. Statistical methods for the analyses in clinical practice. Part 1. Univariate statistical analysis. *Probl Endokrinol*. 2009;55(5):48-55 (in Russian). https://doi.org/10.14341/probl200955548-55
20. Lutz NW, Bernard V. Contactless thermometry by MRI and MRS: Advanced methods for thermotherapy and biomaterials. *iScience*. 2020;23:e101561. https://doi.org/10.1016/j.isci.2020.101561
21. Cohen E, Ahmed O, Kocherginsky M, et al. Study of functional infrared imaging for early detection of mucositis in locally advanced head and neck cancer treated with chemoradiotherapy. *Oral Oncol*. 2013;49(10):1025-1031. https://doi.org/10.1016/j.oraloncology.2013.07.009
22. Shustakova GV, Fomenko YuV, Gordiyenko EYu, et al. Application of infrared thermal imaging for monitoring and prediction of mucositis grade in the course of radiotherapy of head/neck tumors. *Ukr J Radiol Oncol*. 2015;23(3):30-37 (in Russian). http://nbuv.gov.ua/UJRN/URLZh_2015_23_3_6

Submitted: March 24, 2023

Л.Г. Мірошниченко [1], Л.Л. Васильєв [1], Г.В. Шустакова [2], Є.Ю. Гордієнко [2], Ю.В. Фоменко [2], І.П. Дунаєва [3]

[1] Державна установа «Інститут медичної радіології та онкології імені С.П. Григор'єва НАМН України», Харків, Україна
[2] Фізико-технічний інститут низьких температур ім. Б.І. Вєркіна НАН України, Харків, Україна,
[3] Харківський національний медичний університет, Харків, Україна

ІНФРАЧЕРВОНА ТЕРМОГРАФІЯ КОНТРОЛЮЄ ДИНАМІКУ РАДІАЦІЙНОГО ДЕРМАТИТУ

Стан питання. Радіаційний дерматит погіршує якість життя онкологічних хворих і може призвести до необхідності переривання променевої терапії. Ступінь дерматиту суб'єктивно оцінюється при візуальному огляді. Існує гостра потреба як в об'єктивному кількісному методі оцінки поточного ступеня дерматиту, так в прогнозуванні його тяжкості на ранній стадії променевої терапії. **Мета.** Оцінити переваги та недоліки інфрачервоної термографії для моніторингу поточного рівня радіаційного дерматиту та прогнозування його тяжкості шляхом кількісного аналізу динаміки теплового поля в зоні опромінення. **Матеріали та методи.** Методом інфрачервоної термографії обстежено 30 дорослих пацієнтів під час курсу 2D традиційної променевої терапії злоякісних пухлин різного типу та локалізації. Застосували розроблений нами підхід до кількісної оцінки теплового поля, викликаного лише дерматитом, і статистичний (кореляційний та ROC) аналіз. **Результати.** У 100% досліджуваних пацієнтів спостерігався дерматит різного ступеня тяжкості. Динаміка інтенсивності аномальних теплових полів в зоні опромінення корелювала з динамікою ступенів дерматиту (за винятком радіочутливої пухлини), коефіцієнт кореляції (0,74÷0,84). Встановлено, що максимум токсичності (дерматит ≥ 3 ступеня) розвивається у пацієнтів, які виявляють значну гіпертермію в зоні інтересу (≥ 0,7 °C) на ранній стадії променевої терапії. Аналіз ROC показав «хорошу якість» методу прогнозування (AUC = 0,871). **Висновки.** Неінвазивна та дешева інфрачервона термографія є придатним інструментом для об'єктивного кількісного моніторингу поточного ступеня дерматиту під час променевої терапії, а також прогнозування його тяжкості для будь-якої локалізації пухлини.

Ключові слова: онкологія, променева терапія, дерматит, термографія.